ISSN 2071-2898 (Print)
ISSN 2071-2901 (Online)

Bragin M.D., Rogov B.V.

A new hybrid scheme for computing discontinuous solutions of hyperbolic equations

Recommended form of bibliographic references: Bragin M.D., Rogov B.V. A new hybrid scheme for computing discontinuous solutions of hyperbolic equations // Keldysh Institute Preprints. 2016. No. 22. 20 p. doi:**10.20948/prepr-2016-22-e**
URL: **http://library.keldysh.ru/preprint.asp?id=2016-22&lg=e**

KELDYSH INSTITUTE OF APPLIED MATHEMATICS
Russian Academy of Sciences

M. D. Bragin, B. V. Rogov

A new hybrid scheme for computing discontinuous solutions of hyperbolic equations

Moscow — 2016

Michael Dmitrievich Bragin, Boris Vadimovich Rogov

A new hybrid scheme for computing discontinuous solutions of hyperbolic equations

In this work, the hybrid scheme is analyzed. It was introduced earlier as a technique to monotonize bicompact schemes for hyperbolic equations and systems. Its imperfections are discussed. They include the disregard of the various behavior of solution components in the general case, monotonizing nature dependence on a system of units and on a scale of initial and boundary conditions; the lack of a priori estimations of the hybrid scheme tuned parameter. To eliminate these imperfections a new hybrid scheme is constructed. It involves the component-wise monotonization and the solution normalization. The correct normalization is obtained. The general algorithm for a priori estimation of the hybrid scheme parameter is proposed. Numerical examples for the hybrid bicompact scheme with the first-order explicit upwind scheme monotonizer are considered.

Keywords: hybrid scheme, bicompact scheme, monotonicity preserving schemes, hyperbolic equations, discontinuous solutions.

This research was supported by the Russian Foundation for Basic Research, project №14-01-00775.

Contents

Introduction

Many models in physics and technology are based on hyperbolic equations and systems of equations. Numerical methods are used to calculate their solutions in the majority of practically interesting cases since analytical methods are either limited or lacking. The problem of constructing reliable high-order numerical methods for hyperbolic equations remains actual nowadays.

It is common for solutions of hyperbolic equations to have strong discontinuities. High-order schemes, however, generate spurious, non-physical oscillations (nonmonotonicities) near discontinuities. Such behavior is called the Gibbs phenomenon [1] and is explained by the well-known Godunov theorem [2]. At the same time, a numerical method should provide an adequate solution which is free of any non-physical features. Therefore, there is a need of a monotonization (e. g. limiting, filtering, weighting ...) of high-order schemes with no substantial loss in their high accuracy.

There exists a large variety of different monotonization techniques at the present time. Let us mention the most popular and (or) the most novel ones.

In [3, 4] special numerical flux limiters are introduced in order to suppress oscillations near discontinuities. Numerical filters are used in [5–8] for monotonization. The classical idea of artificial viscosity [9] is developed in [10–13]. One often employs a scheme, in which compact Hermit interpolations on candidate stencils are used to compute fluxes at cell faces, and then either ENO algorithm [14] is used to choose a proper stencil or WENO algorithm [15–20] is used to compute weighting coefficients of compact interpolations on candidate stencils.

Recently, hybrid schemes were proposed in [21–25]. They develop the ideas of R. P. Fedorenko [26]. The transition operator of a hybrid scheme is constructed as a nonlinear convex combination of transition operators of a monotone first-order scheme and a non-monotone high-order scheme. The key difference between hybrid schemes transition operator and other similar operators is that it is totally local: the solution of a hybrid scheme depends on values of partner schemes solutions only at the current spatiotemporal point. The technique for constructing hybrid schemes [21, 27] was successfully used to monotonize a non-central multioperator scheme of ninth-order accuracy in space and fourth-order accuracy in time [28].

In this work, a new hybrid scheme is proposed which eliminates imperfections of hybrid schemes [21–25] The work is organized as follows. In Section 1 the hybrid scheme from [24] is analyzed (it is similar to those in [21–23, 25]) and its imperfections are revealed. In Section 2 the new hybrid scheme is proposed. This new hybrid scheme eliminates the imperfections from Section 1. In Section 3

the correct normalization for the new hybrid scheme is found. In addition, a numerical example is considered, where the correct normalization is compared with normalizations from [25]. In Section 4 the problem of a priori estimation of the hybrid scheme tuned parameter C_1 is discussed.

1. The original hybrid scheme and its imperfections

Let us analyze the original hybrid scheme [24] and reveal some of its imperfections connected with the construction of the weighting coefficient. We shall also call this scheme *the old hybrid scheme*. First, let us describe the technique for constructing this scheme in the most general case.

Consider the following system of multidimensional quasilinear hyperbolic equations:

$$\partial_t \mathbf{Q} + \sum_{k=1}^{d} \partial_{x_k} \mathbf{F}_k(\mathbf{Q}) = \mathbf{S}(\mathbf{x}, t, \mathbf{Q}), \quad \mathbf{x} = (x_1, \ldots, x_d) \in D, \quad 0 < t \leqslant T. \tag{1}$$

Here $\mathbf{Q} = (\mathrm{Q}_1, \ldots, \mathrm{Q}_m) = \mathbf{Q}(\mathbf{x}, t) \in \mathbb{R}^m$ is the unknown vector of conservative variables, $\mathbf{F}_k$ are flux vectors, $\mathbf{S}$ is the vector of source terms, $D \subset \mathbb{R}^d$ is the computational domain. System (1) is supposed to be complemented with some conditions that include an initial condition at $t = 0$ and a boundary condition at the boundary ∂D of the domain D. Assume that a unique solution of the mixed problem described above exists in $\{\mathbf{x} \in \overline{D},\ 0 \leqslant t \leqslant T\}$ where $\overline{D} = D \cup \partial D$.

Suppose the mixed problem for system (1) is solved numerically using two schemes, both one-step in time: a monotone first-order scheme A and a non-monotone high-order scheme B. Also, the spatial grid $\Omega = \{\mathbf{x}_j\}_{j=0}^{N_\mathbf{x}}$ is introduced in the closed domain $\overline{D}$ and the time interval $[0, T]$ is split (maybe non-uniformly) by levels t^n $(n = 0, \ldots, N_t)$, $t^0 = 0$, $t^{N_t} = T$. The time step is denoted by $\tau = \tau^{n+1} = t^{n+1} - t^n$. In the text below the upper index $n + 1$ is omitted for brevity.

Assume the solution $\mathbf{Q}^n$ at the time level t^n is known. Let us use it as an initial value for schemes A and B and compute independently their solutions $\mathbf{Q}_A^{n+1}$ and $\mathbf{Q}_B^{n+1}$ respectively at the level t^{n+1}. The resulting solution at the level t^{n+1} at each node $\mathbf{x}_j$ of the grid Ω is computed then using the formula

$$\mathbf{Q}^{n+1}(\mathbf{x}_j) = \alpha(\mathbf{x}_j)\mathbf{Q}_A^{n+1}(\mathbf{x}_j) + (1 - \alpha(\mathbf{x}_j))\mathbf{Q}_B^{n+1}(\mathbf{x}_j) \tag{2}$$

where the weighting coefficient α at the node $\mathbf{x}_j$ is given by

$$\alpha(\mathbf{x}_j) = f(w(\mathbf{x}_j)), \quad w(\mathbf{x}_j) = \frac{C_1 \|\mathbf{Q}_A^{n+1}(\mathbf{x}_j) - \mathbf{Q}_B^{n+1}(\mathbf{x}_j)\|_\infty}{\tau}. \tag{3}$$

The norm in formula (3) is taken not along space, but in components of the difference $\mathbf{Q}_A^{n+1} - \mathbf{Q}_B^{n+1}$ at the node $\mathbf{x}_j$. Therefore, the weighting coefficient α may generally take on different values at different nodes of the grid Ω. The function $f(w)$ is supposed to be known; it is determined on the whole semi-axis $w \geqslant 0$ and must meet the following requirements:

1) $0 \leqslant f(w) \leqslant 1$ for all $w \geqslant 0$ (combination (2) is convex);
2) $f(0) = 0$, $f(+\infty) = 1$, $f(w)$ is monotone nondecreasing for $w \geqslant 0$;
3) $f(w) = \mathrm{const} \cdot w^q + o(w^q)$ when $w \to 0$ where $q \geqslant p - 1$ and p is order of accuracy of scheme B.

For example, one may choose the function $f(w)$ as the

$$f(w) = \frac{w^q}{1 + w^q}, \quad q \geqslant p - 1. \tag{4}$$

Function (4) belongs to $C^\infty[0, +\infty)$. The quantity $C_1 = \mathrm{const} > 0$ is the single tuned parameter of the hybrid scheme. Parameter C_1 depends on the problem solved (i. e. on actual expressions for $\mathbf{F}_k$ and $\mathbf{S}$, on initial and boundary conditions) and on the choice of schemes A, B.

Let us explain the meaning of formula (2). Where the exact solution $\mathbf{Q}_E(\mathbf{x}, t)$ of the mixed problem for system (1) is smooth, the difference between A and B solutions is small, $\alpha \approx 0$ and $\mathbf{Q}^{n+1} \approx \mathbf{Q}_B^{n+1}$. Where $\mathbf{Q}_E(\mathbf{x}, t)$ changes abruptly or shockwise, the scheme B generates spurious, non-physical oscillations (the Gibbs phenomenon), the difference between A and B solutions is large (since the scheme A is monotone), $\alpha \approx 1$ and $\mathbf{Q}^{n+1} \approx \mathbf{Q}_A^{n+1}$.

Note that if the function f is chosen as function (4), the scheme B shall still be monotonized even in smoothness regions of the exact solution since $f(w) = 0$ only at $w = 0$. However, this fact does not result into an accuracy reduction of the hybrid scheme in such regions. To show this, let us rewrite formula (2) in the form

$$\mathbf{Q}^{n+1}(\mathbf{x}_j) = \\ = \mathbf{Q}_B^{n+1}(\mathbf{x}_j) + \alpha(\mathbf{x}_j) \left(\mathbf{Q}_A^{n+1}(\mathbf{x}_j) - \mathbf{Q}_B^{n+1}(\mathbf{x}_j) \right) = \mathbf{Q}_B^{n+1}(\mathbf{x}_j) + \mathbf{Z}^{n+1}(\mathbf{x}_j)$$

where $\mathbf{Z}^{n+1}(\mathbf{x}_j) = \alpha(\mathbf{x}_j) \left(\mathbf{Q}_A^{n+1}(\mathbf{x}_j) - \mathbf{Q}_B^{n+1}(\mathbf{x}_j) \right)$. Because of the exact solution smoothness, expression (3) for the weighting coefficient and the third property of the function f we have $\mathbf{Z}^{n+1} \sim \tau^q \cdot \tau^2 \leqslant \tau^{p+1}$, i. e. the addition to the solution $\mathbf{Q}_B^{n+1}$ of scheme B is negligibly small in comparison to the B's approximation error. Therefore, if the function f is chosen as function (4), the accuracy of the hybrid scheme shall not reduce to the accuracy of the scheme A in smoothness regions of the exact solution, which was to be shown.

It is important to note that hybrid scheme formula (2) includes only quantities taken at the current spatiotemporal point $(\mathbf{x}_j, t^{n+1})$. From this viewpoint

formula (2) is totally local. It does not involve neighboring nodes neither in $\mathbf{x}$, nor in t. That is why the construction of hybrid scheme is versatile in sense of D geometry or the grid Ω. The grid can be either structured or unstructured. It is easy to see that the form of equations in system (1) also does not affect the notation of hybrid scheme (2): left-hand sides of equations in system (1) can be written in a non-conservative form; system coefficients can depend on $\mathbf{x}$ and t and so on. Neither a choice of schemes A and B, nor their stencils have any effect on the hybrid scheme notation. These properties make the hybrid scheme to stand out among other monotonization methods mentioned in the Introduction.

Nevertheless, all the factors listed in the paragraph above determine the choice of the parameter C_1; the particular function f depends on the B's order of accuracy. The constant C_1 is recommended to be found by the method of successive approximations during preliminary calculations on coarse grids.

Now let us discuss the construction of the weighting coefficient α (see (3)). It has a number of imperfections.

The first imperfection: all components $\mathrm{Q}_{Ai}, \mathrm{Q}_{Bi}$ $(i = 1, \ldots, m)$ of vectors $\mathbf{Q}_A, \mathbf{Q}_B$ at the point $(\mathbf{x}_j, t^{n+1})$ are weighted with the same weight $\alpha(\mathbf{x}_j)$. For instance, assume that in a neighborhood of the point $\mathbf{x}_j$ some components change smoothly, while others change sharply. Then, even the smoothly changing components are monotonized although there is no need for them to be monotonized. This can be seen from formula (3): the norm $\|\mathbf{Q}_A^{n+1}(\mathbf{x}_j) - \mathbf{Q}_B^{n+1}(\mathbf{x}_j)\|_\infty$ is reached on a "discontinuous" component, the weight $\alpha(\mathbf{x}_j)$ is not close to 0, and the "continuous" components are monotonized substantially and undesirable. For example, the norm $\|.\|_\infty$ may be replaced with norms $\|.\|_1, \|.\|_2, \ldots$, but that shall not change the situation in the main. A suitable initial condition can always be chosen in a way that the number i_0 exists, for which

$$|\mathrm{Q}_{Ai_0}(\mathbf{x}_j, t^{n+1}) - \mathrm{Q}_{Bi_0}(\mathbf{x}_j, t^{n+1})| \gg \\ \gg (m-1)|\mathrm{Q}_{Ai}(\mathbf{x}_j, t^{n+1}) - \mathrm{Q}_{Bi}(\mathbf{x}_j, t^{n+1})|, \quad i \neq i_0$$

(the large "discontinuity" of the component i_0) and norms $\|.\|_1, \|.\|_2, \ldots$ shall be reduced to the norm $\|.\|_\infty$.

One may face the first imperfection in the following practical case: system (1) is the Euler gas dynamics equations, their solution is a large contact discontinuity, and the primitive variables U_i (density, velocity, pressure) are used instead of conservative variables Q_i (density, mass flux, energy per unit volume). In a neighborhood of the contact the large jump in density shall result into the monotonization of pressure at the same place though pressure is changing continuously.

The second imperfection: the difference $\mathbf{Q}_A^{n+1}(\mathbf{x}_j) - \mathbf{Q}_B^{n+1}(\mathbf{x}_j)$ enters the formula for the argument $w(\mathbf{x}_j)$ in (3) without any kind of normalization. Though

the presence of the component norm means indirectly that system (1) has been already nondimensionalized, i. e. $[\mathrm{Q}_i] = 1$ $(i = 1, \ldots, m)$[1], any other choice of dimensional scales or a variation of the initial/boundary conditions range in non-dimensional units shall make all α weights at all nodes $\mathbf{x}_j \in \Omega$ to change. It shall be so if the constant C_1 remains unvaried. Therefore, one needs to either re-calculate C_1 or accept a new monotonization behavior. The first seems to be inconvenient while the last seems to be unreasonable.

The presence of τ in formula (3) is questionable. The statement that the parameter C_1 can be estimated during preliminary calculations on coarse grids is correct until the relation $r = \tau/h$ changes weakly when the grid is refined. Here h is the typical linear scale of the spatial grid Ω. (If the grid Ω is cartesian, then $h = \max(h_1, \ldots, h_d)$ where $h_1, \ldots, h_d$ are $Ox_1, \ldots, Ox_d$ axises steps respectively.)

The third imperfection: the necessity of selecting the constant C_1 for every single problem. One would like to have some sort of an "optimal" value of the parameter C_1 found in not even the general case, but in some special (toy) cases (e. g. the simple one-dimensional linear advection equation, the one-dimensional gas dynamics). Of course, it shall not be strictly applicable in the general case. This value shall be enough within engineer accuracy or shall serve as a good initial approximation for the step-by-step choice of C_1 in a particular problem.

Thus, our purpose shall be an elimination of the imperfections listed above.

2. The new hybrid scheme

Let us construct a new scheme in a way which eliminates the imperfections of the old hybrid scheme. The first and the second imperfections are eliminated in a quite simple way which is already contained in their description. To avoid the first imperfection the vector weighting should be replaced with the component-wise weighting. The second imperfection is solved by introducing a proper normalization and by removing τ from the formula for the argument w.

Taking these notes into account, we rewrite the old hybrid scheme (see (2)–(3)): at each node $\mathbf{x}_j$ of the grid Ω for all $i = 1, \ldots, m$

$$\mathrm{Q}_i^{n+1}(\mathbf{x}_j) = \alpha_i(\mathbf{x}_j)\mathrm{Q}_{Ai}^{n+1}(\mathbf{x}_j) + (1 - \alpha_i(\mathbf{x}_j))\mathrm{Q}_{Bi}^{n+1}(\mathbf{x}_j) \tag{5}$$

where the weighting coefficient

$$\alpha_i(\mathbf{x}_j) = f(w_i(\mathbf{x}_j)), \quad w_i(\mathbf{x}_j) = \frac{C_1|\mathrm{Q}_{Ai}^{n+1}(\mathbf{x}_j) - \mathrm{Q}_{Bi}^{n+1}(\mathbf{x}_j)|}{\mathcal{N}(\mathrm{Q}_{Ai}^{n+1})}. \tag{6}$$

[1]Hereafter square brackets mean the dimension of a quantity.

Here $\mathcal{N}(.)$ is the functional which determines the *normalization* as it was called above. It assigns a positive number to each scalar function determined on the grid Ω. Let us call hybrid scheme (5)–(6) as *the new hybrid scheme*.

It is easy to see that both the old and the new hybrid schemes have the same working principle. When the function f is chosen as (4), the accuracy of the new hybrid scheme does not reduce to the A's accuracy in smoothness areas of the exact solution, as it is shown in Section 1. The new hybrid scheme inherits all positive properties of the old one including locality. The correction done in formulas (5)–(6) is not qualitative but quantitative. This modification makes the monotonization more accurate since only "discontinuous" components of the numerical solution are monotonized.

In order to eliminate the second imperfection completely, one should find the normalization $\mathcal{N}(.)$ which always transforms Q_{Ai}^{n+1}'s and Q_{Bi}^{n+1}'s value ranges (approximately for Q_{Bi}^{n+1} because of its nonmonotonicities) into the standard closed interval $[0, 1]$.

3. The correct normalization

Let us solve the problem of choosing the normalization $\mathcal{N}(.)$. This problem was formulated at the end of the previous Section.

Assume ξ, η are some quantities that vary in the range $[a, b]$. Then quantities

$$\xi' = \frac{\xi - a}{b - a}, \quad \eta' = \frac{\eta - a}{b - a}$$

vary in the range $[0, 1]$. Consider their difference $\xi' - \eta'$:

$$\xi' - \eta' = \frac{\xi - \eta}{b - a} \in [-1, 1],$$

and its absolute value

$$|\xi' - \eta'| = \frac{|\xi - \eta|}{b - a} \in [0, 1].$$

Therefore we obtain the desired normalization

$$\mathcal{N}_{\mathrm{span}}(\mathrm{Q}_{Ai}^{n+1}) = \max_{\Omega} \mathrm{Q}_{Ai}^{n+1} - \min_{\Omega} \mathrm{Q}_{Ai}^{n+1}. \tag{7}$$

Note $\mathcal{N}_{\mathrm{span}}(\mathrm{const}) = 0$. It is clear that the functional $\mathcal{N}_{\mathrm{span}}(.)$ is a semi-norm in the linear space of mesh functions determined on Ω.

Earlier the global and the local normalizations were proposed in [25]. The global normalization is

$$\mathcal{N}_{\mathrm{global}}(\mathrm{Q}_{Ai}^{n+1}) = \|\mathrm{Q}_{Ai}^{n+1}\|_{\infty} = \max_{\Omega} |\mathrm{Q}_{Ai}^{n+1}| \tag{8}$$

and the local is

$$\mathcal{N}_{\mathrm{local},\,\mathbf{x}_j}(\mathrm{Q}_{Ai}^{n+1}) = |\mathrm{Q}_{Ai}^{n+1}(\mathbf{x}_j)|. \tag{9}$$

The local normalization (9) differs from the one considered in [25]. It is written in a form which allows to use this normalization for the arbitrary grid Ω and for arbitrary geometries of the domain D. This difference does not change the nature of the normalization. Note that functional $\mathcal{N}_{\mathrm{local},\,\mathbf{x}_j}(.)$ values depends not only on the mesh function but also on the grid node where this functional is computed.

Let us write the expressions for the weighting coefficient argument (6) that correspond to normalizations (7), (8), (9). If $\mathcal{N} = \mathcal{N}_{\mathrm{span}}$,

$$w_i(\mathbf{x}_j) = \frac{C_1|\mathrm{Q}_{Ai}^{n+1}(\mathbf{x}_j) - \mathrm{Q}_{Bi}^{n+1}(\mathbf{x}_j)|}{\max\limits_{\Omega} \mathrm{Q}_{Ai}^{n+1} - \min\limits_{\Omega} \mathrm{Q}_{Ai}^{n+1} + \varepsilon_{\mathrm{m}}}. \tag{10}$$

If $\mathcal{N} = \mathcal{N}_{\mathrm{global}}$,

$$w_i(\mathbf{x}_j) = \frac{C_1|\mathrm{Q}_{Ai}^{n+1}(\mathbf{x}_j) - \mathrm{Q}_{Bi}^{n+1}(\mathbf{x}_j)|}{\max\limits_{\Omega} |\mathrm{Q}_{Ai}^{n+1}| + \varepsilon_{\mathrm{m}}}. \tag{11}$$

If $\mathcal{N} = \mathcal{N}_{\mathrm{local},\,\mathbf{x}_j}$,

$$w_i(\mathbf{x}_j) = \frac{C_1|\mathrm{Q}_{Ai}^{n+1}(\mathbf{x}_j) - \mathrm{Q}_{Bi}^{n+1}(\mathbf{x}_j)|}{|\mathrm{Q}_{Ai}^{n+1}(\mathbf{x}_j)| + \varepsilon_{\mathrm{m}}}. \tag{12}$$

The quantity ε_{m} is a small positive number which prevents from dividing by zero (e. g. a "machine precision").

Unlike normalization (7), normalizations (8) and (9) do not avoid troubles. They both are "vulnerable" to any shift of the Q_{Ai}^{n+1}'s value range. Let us demonstrate this on the following example. Consider two variants of initial/boundary conditions for system (1). Assume the index i and the moment of time t_0 are fixed. Suppose there is a discontinuity of the component i in some part of D at $t = t_0$. Let Q_{Ei} take on values q_1, q_2 at sides of the discontinuity for the first variant and values $q_1 + \Delta q$, $q_2 + \Delta q$ for the second variant. The addition $\Delta q > 0$ and $\Delta q \gg |q_1 - q_2|$. Let $\|\mathrm{Q}_{Ei}|_{t=t_0}\|_\infty \sim \max(|q_1|, |q_2|)$. Turn now to the time level $t^{n+1} = t_0$. Then weighting coefficient distributions across the discontinuity are different for these two variants of conditions. In the second variant these weights are smaller since arguments $w_i(\mathbf{x}_j)$ are smaller because of the addition Δq in the denominator and since properties of the function f. Therefore, nonmonotonicities in the second variant are greater in comparison with those in the first variant. Thus, a simple translation of value range leads to a change in monotonization behavior. It is absolutely unreasonable since the scale $|q_1 - q_2|$ of the discontinuity is the same for both variants. Let us add that if $q_1 \approx 0$ or $q_2 \approx 0$ then local normalization shall produce huge numerical dissipation near the discontinuity front.

Consider the simplest special case of system (1) — the one-dimensional homogeneous scalar linear advection equation

$$\partial_t u + a\,\partial_x u = 0, \quad a = \text{const} > 0, \quad x > 0, \quad 0 < t \leqslant T, \tag{13}$$

$$(d = 1, \quad \mathbf{x} = x_1 = x, \quad D = (0, +\infty), \quad \mathbf{Q} = u, \quad \mathbf{F}_1 = au, \quad \mathbf{S} = 0),$$

where $u = u(x, t)$ is the unknown function. Also, we examine 4 variants of initial and boundary conditions for equation (13). Let us call them *tests*.

Test 1:

$$u|_{t=0} = \begin{cases} 1, & x < x_s, \\ 0, & x \geqslant x_s, \end{cases} \quad x \geqslant 0; \quad u|_{x=0} = 1, \quad 0 < t \leqslant T. \tag{14}$$

Test 2:

$$u|_{t=0} = \begin{cases} 10^6, & x < x_s, \\ 0, & x \geqslant x_s, \end{cases} \quad x \geqslant 0; \quad u|_{x=0} = 10^6, \quad 0 < t \leqslant T. \tag{15}$$

Test 3:

$$u|_{t=0} = \begin{cases} 1001, & x < x_s, \\ 1000, & x \geqslant x_s, \end{cases} \quad x \geqslant 0; \quad u|_{x=0} = 1001, \quad 0 < t \leqslant T. \tag{16}$$

Test 4:

$$u|_{t=0} = \begin{cases} 2 \cdot 10^6, & x < x_s, \\ 10^6, & x \geqslant x_s, \end{cases} \quad x \geqslant 0; \quad u|_{x=0} = 2 \cdot 10^6, \quad 0 < t \leqslant T. \tag{17}$$

Denote by $u_{1,2,3,4}(x, t)$ solutions of equation (13) complemented with conditions (14)–(17) respectively. At each point $(x, t) \in \{0 \leqslant x < +\infty,\ 0 \leqslant t \leqslant T\}$ these solutions satisfy the equality

$$u_1(x, t) = \frac{u_2(x, t)}{10^6} = u_3(x, t) - 1000 = \frac{u_4(x, t)}{10^6} - 1 \tag{18}$$

whether they are obtained analytically or numerically using an arbitrary linear scheme for (13). Obviously this equality is a consequence of the superposition principle which is true for linear equations and schemes.

Let us clarify the meaning of these tests. Test 1 is about a standard monotone nonincreasing "jump" of unit amplitude. In tests 2–4 this "jump" is a subject to the following linear transformations at $t = 0$: in test 2 it is scaled by 10^6 times, in test 3 it is translated by 1000 and in test 4 it is both translated by 1 and scaled by 10^6 times.

Using tests 1–4 as the examples, let us show the work of normalizations (7)–(9) as well as the work of the normalization $\mathcal{N}_{\text{no}} \equiv 1$ (it means no normalization and corresponds to the old hybrid scheme). The scheme A is the first-order explicit upwind scheme, the scheme B is the bicompact scheme [24]. The time integration method used in the bicompact scheme is the L-stable stiffly accurate diagonally implicit Runge–Kutta method of the 3rd order (see its Butcher's tableau (20) in [24]). Parameters are chosen as

$$a = 1, \quad T = 1, \quad x_s = 1, \quad h = 0.01, \quad \kappa = 0.4, \quad C_1 = 100$$

where $\kappa = a\tau/h$ is the Courant number. The parameter $q = 2$ in the function f (4). Half-integer nodes in the scheme B are treated as integer by the scheme A. Particularly, the Courant number for the scheme A is equal to 2κ, not κ.

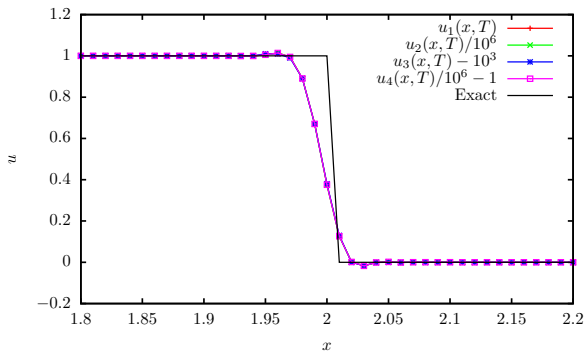

Fig. 1. Solutions of tests 1–4 obtained using the new hybrid scheme with $\mathcal{N}_{\text{span}}$

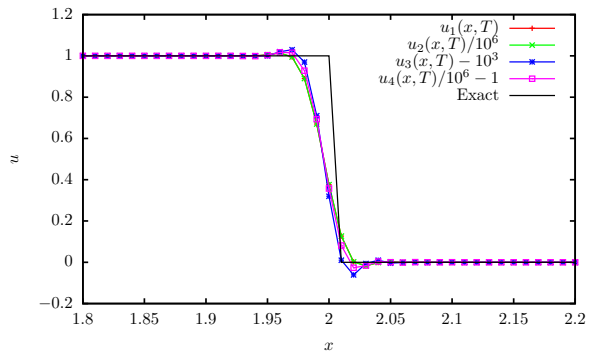

Fig. 2. Solutions of tests 1–4 obtained using the new hybrid scheme with $\mathcal{N}_{\text{global}}$

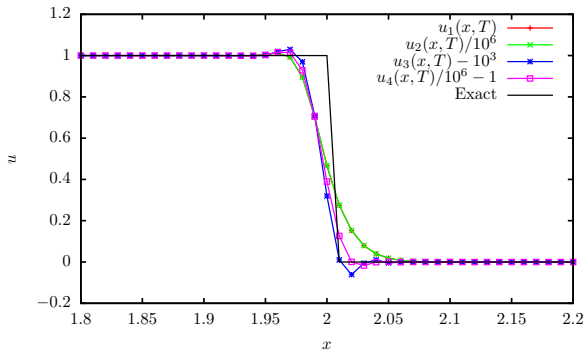

Fig. 3. Solutions of tests 1–4 obtained using the new hybrid scheme with $\mathcal{N}_{\text{local}}$

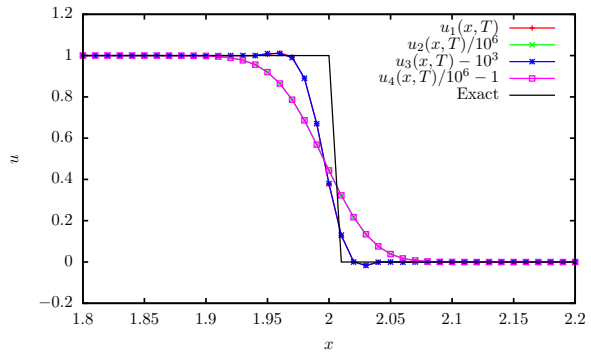

Fig. 4. Solutions of tests 1–4 obtained using the new hybrid scheme with $\mathcal{N}_{\text{no}}$

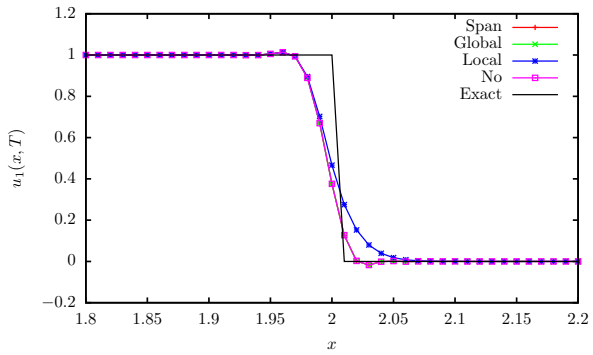

Fig. 5. Solutions obtained using the new hybrid scheme with various normalizations, test 1

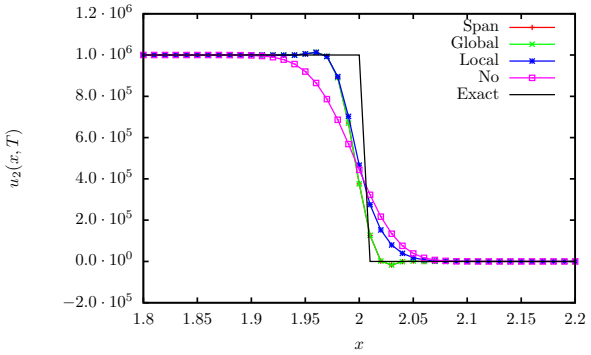

Fig. 6. Solutions obtained using the new hybrid scheme with various normalizations, test 2

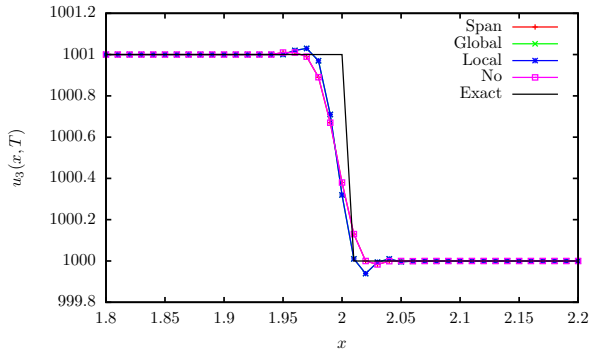

Fig. 7. Solutions obtained using the new hybrid scheme with various normalizations, test 3

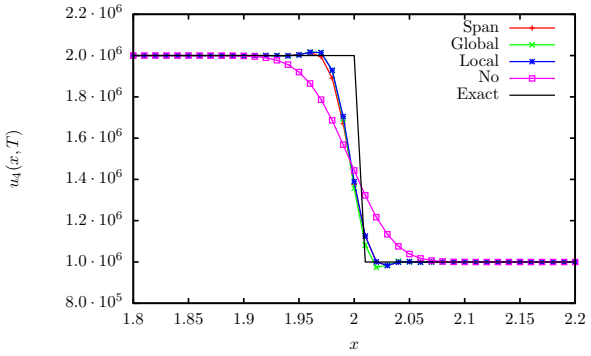

Fig. 8. Solutions obtained using the new hybrid scheme with various normalizations, test 4

Solution profiles $u_{1,2,3,4}(x,T)$ are presented on Fig. 1–4. The solutions are obtained using the new hybrid scheme. On each figure the normalization is fixed while tests are varied. Ranges of the solutions are transformed into the range $[0,1]$ according to equalities (18). It can be seen well on Fig. 1 that the normalization $\mathcal{N}_{\text{span}}$ is stable to linear transformations of the solution range just as it was expected. Therefore, the formally nonlinear new hybrid scheme with $\mathcal{N}_{\text{span}}$ inherits this property of linear schemes. Let us turn to Fig. 2, 3. It is clear that both the global and the local normalizations are insensitive to solution range scalings but they are sensitive to translations as it was mentioned above. It can be seen also that the larger translation is, the smaller weighting coefficients are. In addition, the solution of the hybrid scheme is closer to the one of the non-monotone scheme B. The scheme with no normalization ignores translations but is sensitive to scalings (see Fig. 4).

Fig. 5–8 depict solution profiles. Again, the solutions are calculated using the new hybrid scheme. Now on every figure normalizations are varied while the test is fixed. These plots allow to analyze differences between $\mathcal{N}_{\text{span}}$ and other normalizations for each test. All normalizations except the local $\mathcal{N}_{\text{local}}$ give similar results in test 1 (see Fig. 5). The local normalization works in other way there because the solution of the scheme A plateaus zero value at $x > 2$, $t = T$. At these points the denominator in the formula for w decreases (see (12)), w itself goes to $+\infty$ and so $f(w) \to 1$. Therefore, the solution of the hybrid scheme suffers from excessive dissipation and goes to the solution of the scheme A. The local normalization behaves similar in test 2 (see Fig. 6). It is clear that a scaling of initial/boundary values results into a scaling of $(u_A - u_B)$. The scheme with no normalization makes all w at all nodes to increase proportionally, all of α go closer to unity, and unnecessary dissipation turns on as a result (see Fig. 6, 8). Note the global and the local normalizations behave in the same way in test 3 (see Fig. 7): a translation results into an underestimation of weighting coefficients (11), (12) at all nodes. There is a lack of dissipation and nonmonotonicities of the scheme B appear.

Thus the correct normalization (10) has been constructed for the new hybrid scheme (5)–(6). Also, the numerical example has been considered. It has showed the work of this normalization and its differences from other normalizations.

4. Finding an optimal value of the parameter C_1

Now let us discuss the problem of finding an "optimal" value of the parameter C_1 (see the third imperfection in Section 1). It is reasonable to consider this problem concerning the typical case of "jump" profile linear advection, namely, test 1 from Section 3.

Two remarks should be made before determining the term "optimal". First, when $C_1 \to +\infty$ the solution of the hybrid scheme goes to solution of the scheme A. Second, with any C_1 the hybrid scheme gives a solution which is not accurately monotone according to the Godunov definition. In the following, we shall use only the Godunov definition of a monotone scheme.

Therefore, the definition of monotonicity should be somehow revised or weakened. Assume the Godunov monotonicity condition is satisfied not absolutely accurate but with some absolute error ε. Then, the *optimal* choice of the parameter C_1 means the following: choose the least C_1 for which the Godunov monotonicity condition is satisfied with the absolute error ε.

For instance, the approximate monotonicity condition for the hybrid bicompact scheme from Section 3 is written at the level t^n as (suppose $u_E(x,t)$ is

monotone nonincreasing for all $0 \leqslant t \leqslant T$)

$$u^n_{j+\frac{1}{2}} - u^n_{j+1} \geqslant -\varepsilon, \quad u^n_j - u^n_{j+\frac{1}{2}} \geqslant -\varepsilon, \quad j = 0, 1, \ldots \tag{19}$$

The optimal C_1:

$$C_1^{\text{opt}} = \inf\{C_1 \colon \text{condition (19) is satisfied at } t = T\}. \tag{20}$$

The equality $t = T$ in (20) is equivalent to the equality $n = N_t$.

It is clear that C_1^{opt} is a function which depends on many arguments:

$$C_1^{\text{opt}} = C_1^{\text{opt}}(A, B, f; \varepsilon, h, \tau, a, T). \tag{21}$$

Assume $[u] = 1$. Then if we do not consider obvious dependence of C_1^{opt} on A, B, and f (hereafter they are not written in the list of arguments), function (21) is determined by four dimensional arguments h, τ, a, T and one non-dimensional ε. Among the dimensional arguments only two have independent dimensions. They are steps h and τ. Let us use the well-known Π theorem [29]. Thus, we obtain that the function C_1^{opt} depends actually on only three non-dimensional arguments: the absolute error ε in the approximate Godunov condition (19), the number of time steps $N_t = T/\tau$, and the Courant number $\kappa = a\tau/h$, i. e.

$$C_1^{\text{opt}} = C_1^{\text{opt}}(\varepsilon, N_t, \kappa). \tag{22}$$

Despite function (22) depends on only three arguments, it is desirable to go further and somehow exclude the Courant number. This is due to the fact that in nonlinear problems the Courant number varies from node to node while the parameter C_1 is taken constant for the whole computation or at least for a time step. It is necessary to have some C_1 estimation which depends only on ε and N_t. Other words, some effective value of the optimal C_1 is required.

Let $\kappa_{1,2}$ (where $\kappa_1 < \kappa_2$) be practically used stability limits of the hybrid scheme. For the hybrid scheme with the first-order explicit upwind monotonizer from Section 3 $\kappa_1 = 0.05$, $\kappa_2 = 0.45$ (they become 0.1, 0.9 respectively for scheme A). Consider two variants of effective value mentioned above: average one

$$\overline{C}_1 = \frac{1}{\kappa_2 - \kappa_1} \int\limits_{\kappa_1}^{\kappa_2} C_1^{\text{opt}}(\varepsilon, N_t, \kappa)\, d\kappa \tag{23}$$

and maximum one

$$C_1^* = \max_{[\kappa_1, \kappa_2]} C_1^{\text{opt}}(\varepsilon, N_t, \kappa). \tag{24}$$

By the construction

$$\overline{C}_1 = \overline{C}_1(\varepsilon, N_t), \quad C_1^* = C_1^*(\varepsilon, N_t).$$

Fig. 9, 10 depict plots of functions $\overline{C}_1(\varepsilon, N_t)$, $C_1^*(\varepsilon, N_t)$ obtained numerically for the hybrid bicompact scheme with the first-order explicit upwind monotonizer and the normalization $\mathcal{N}_{\text{span}}$. Let us describe the technique of the numerical calculation of $\overline{C}_1$ and C_1^*.

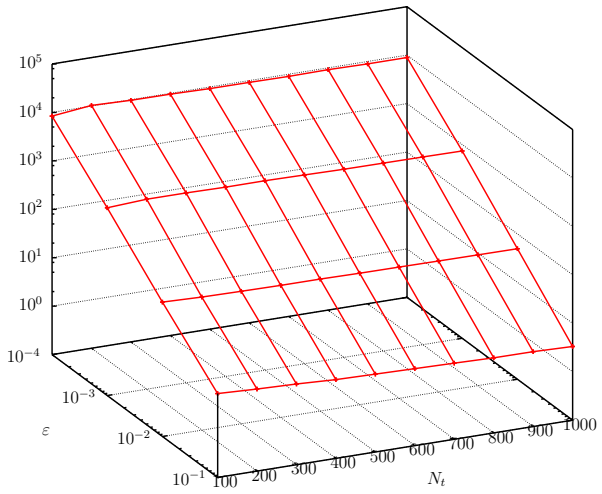

Fig. 9. The function $\overline{C}_1(\varepsilon, N_t)$

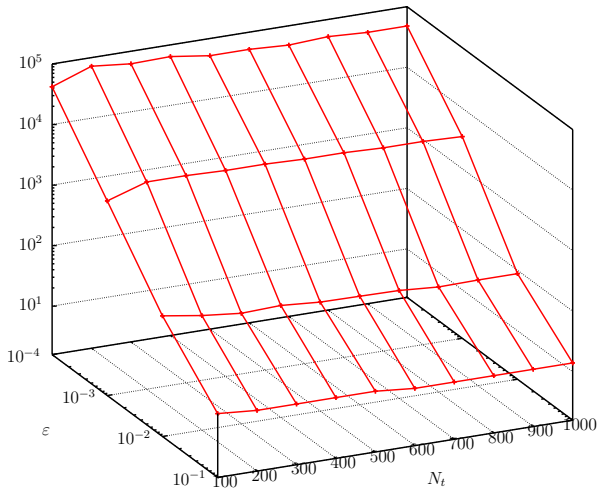

Fig. 10. The function $C_1^*(\varepsilon, N_t)$

The closed interval $[\kappa_1, \kappa_2]$ is discretized using a uniform grid which consists of nodes θ_l ($l = 0, \ldots, N_\kappa$; the number N_κ was equal to 100 during calculations). The point (ε, N_t) is fixed. Next, $C_1^{\text{opt}}(\varepsilon, N_t, \theta_l)$ is found for the set of arguments $(\varepsilon, N_t, \theta_l)$. The search is conducted in the following way. First, $C_1 = 2$ is taken, test 1 is computed using the hybrid scheme with parameters ε, N_t, θ_l, C_1. After that, condition (19) is checked: if it is satisfied then $C_1^{\text{opt}} = C_1$, else C_1 increases by ΔC_1 and the procedure repeats. The increment ΔC_1 is variable:

$$\Delta C_1 = \begin{cases} 2 & \text{if } 2 \leqslant C_1 < 200, \\ 20 & \text{if } 200 \leqslant C_1 < 2000, \\ 200 & \text{if } 2000 \leqslant C_1 < 20000, \\ \ldots & \end{cases}$$

Finally, sought values $\overline{C}_1$ and C_1^* are approximately calculated according to their definitions (23) and (24):

$$\overline{C}_1 \approx \frac{1}{N_\kappa + 1} \sum_{l=0}^{N_\kappa} C_1^{\text{opt}}(\varepsilon, N_t, \theta_l), \quad C_1^* \approx \max_l C_1^{\text{opt}}(\varepsilon, N_t, \theta_l).$$

Note that in real computer calculations the index j can not run to infinity, actually $j = 0, \ldots, N_x$. In other words, x varies between 0 and some L. However, if L is sufficiently great, then it is not in the list of governing parameters in

formula (21) since at $t = T$ the solution of the hybrid scheme (and ones of schemes A and B) plateaus zero quickly enough. In test 1, the jump finds itself at the point $x = x_s + aT$ at $t = T$. The initial position x_s of the jump also plays no part, for instance, let $x_s = aT$. Then, $L = 3aT$ is sufficient. At last, express N_x in terms of κ and N_t:

$$\kappa = \frac{a\tau}{h} = a\frac{T/N_t}{L/N_x} = \frac{N_x}{3N_t}; \quad N_x = 3\kappa N_t.$$

Let us analyze the results that are presented on Fig. 9, 10. It can be seen well, that effective values $\overline{C}_1$ and C_1^* of the parameter C_1 do not depend on N_t practically and do linearly (in logarithmic scale) depend on ε. Very weak dependence on N_t and deviations from linearity in ε for C_1^* can be explained apparently by a rough choice of ΔC_1. The choice of ΔC_1 is less important for $\overline{C}_1$ because of the averaging which smooths errors in calculating C_1^{opt} for given ε, N_t, θ_l.

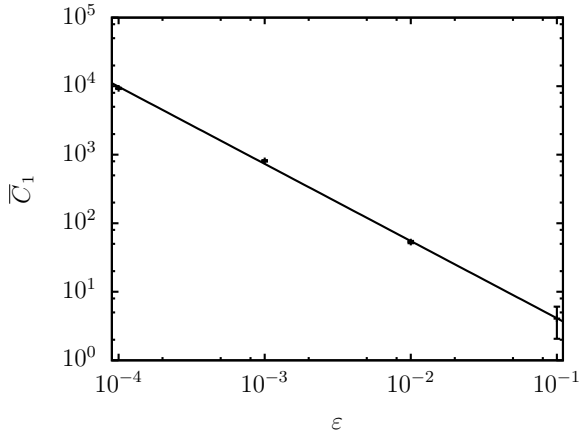

Fig. 11. The function $\overline{C}_1(\varepsilon, 500)$, the solid line depicts the minimum squares method approximation

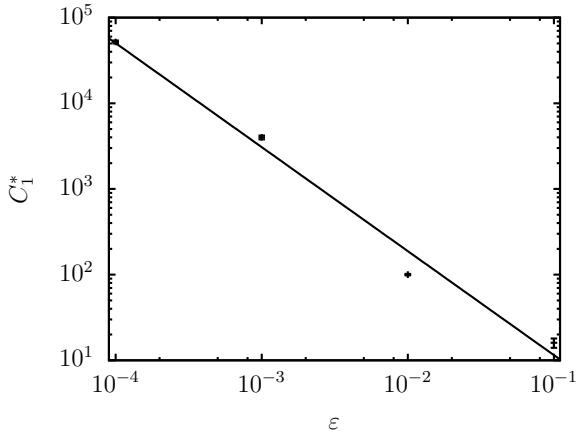

Fig. 12. The function $C_1^*(\varepsilon, 500)$, the solid line depicts the minimum squares method approximation

Fig. 11, 12 represent cuts of $\overline{C}_1(\varepsilon, N_t)$, $C_1^*(\varepsilon, N_t)$ plots at the plane $N_t = 500$ (points with error bars) as well as their minimum squares approximations (solid lines). These approximations appeared to be

$$\overline{C}_1(\varepsilon) = 0.3076 \cdot \varepsilon^{-1.126}, \quad C_1^*(\varepsilon) = 0.7015 \cdot \varepsilon^{-1.214}. \tag{25}$$

Thus, we have solved the problem of finding the parameter C_1 for the hybrid bicompact scheme with the first-order explicit upwind monotonizer. We have obtained explicit formulas (25) that can be used to calculate C_1 depending on ε. The parameter ε has a clear meaning. Maximum tolerable nonmonotonicities in integer nodes can not be greater by their relative value than 2ε.

The ideas of this Section can be extended on the case of arbitrary schemes A and B. Let us give the algorithm (test 1 is the toy problem again):

1) Choose the monotone scheme A.
2) Choose the high-order scheme B. Find p, its order of approximation. Choose the function f using formula (4), taking $q = p - 1$.
3) Construct the hybrid scheme using formulas (5), (6), (7). Find $\kappa_{1,2}$.
4) According to schemes A and B specifics, formulate the approximate Godunov monotonicity condition similar to (19).
5) Calculate functions $\overline{C}_1(\varepsilon, N_t)$, $C_1^*(\varepsilon, N_t)$ either analytically or numerically.

Then, in a real problem the parameter C_1 is estimated using the function $\overline{C}_1(\varepsilon, N_t)$ or $C_1^*(\varepsilon, N_t)$. Numbers ε and N_t are supposed to be given beforehand. Finally, one is either satisfied with this estimation or makes it more precise during some tests on coarse grids (if it is possible).

Concluding remarks

The old hybrid scheme [24] has been analyzed. Its three imperfections have been revealed. The first imperfection is the vector weighting which makes all solution components to be weighted with the same weight. The second imperfection is the sufficient and spurious dependence of the motonizing nature on a choice of system of units and (or) on a initial/boundary values amplitude. The third imperfection is the necessity of choosing the tuned parameter with no a priori estimations available.

The new hybrid scheme has been proposed. It includes the normalization and the component-wise weighting. This scheme does not have the first imperfection by the construction. The correct normalization has been found for the new hybrid scheme which eliminated also the second imperfection. The a priori estimation of the hybrid scheme parameter has been proposed. The estimation depends on a limit of nonmonotonicities amplitudes and on a number of time steps. Therefore, the third imperfection has been eliminated. The hybrid bicompact scheme with the first-order explicit upwind scheme monotonizer has been considered as an example. It has been shown, that in the case of this scheme the proposed estimation does not depend on the number of time steps. Explicit formulas has been found that allow to calculate the hybrid scheme tuned parameter straightaway.

Bibliography list

1. Lax P. D. Gibbs phenomena // J. Sci. Comput. — 2006. — Vol. 28, no. 2/3. — P. 445–449.

2. Godunov S. K. A difference method for numerical calculation of discontinuous solutions of the equations of hydrodynamics // Mat. Sb. (N. S.). — 1959. — Vol. 47 (89), no. 3. — P. 271–306.

3. Cockburn B., Shu C.-W. Nonlinearly stable compact schemes for shock calculations // SIAM J. Numer. Anal. — 1994. — Vol. 31, no. 3. — P. 607–627.

4. Yee H. C. Explicit and implicit multidimensional compact high-resolution shock-capturing methods: Formulation // J. Comput. Phys. — 1997. — Vol. 131, no. 1. — P. 216–232.

5. Ekaterinaris J. A. Implicit, high-resolution, compact schemes for gas dynamics and aeroacoustics // J. Comput. Phys. — 1999. — Vol. 156, no. 2. — P. 272–299.

6. Yee H. C., Sandham N. D., Djomehri M. J. Low-dissipative high-order shock-capturing methods using characteristic-based filters // J. Comput. Phys. — 1999. — Vol. 150, no. 1. — P. 199–238.

7. Yee H. C., Sjögreen B. Adaptive filtering and limiting in compact high order methods for multiscale gas dynamics and MHD systems // Comput. Fluids. — 2008. — Vol. 37, no. 5. — P. 593–619.

8. Darian H. M., Esfahanian V., Hejranfar K. A shock-detecting sensor for filtering of high-order compact finite difference schemes // J. Comput. Phys. — 2011. — Vol. 230, no. 3. — P. 494–514.

9. Von Neumann J., Richtmyer R. D. A method for the numerical calculation of hydrodynamic shocks // J. Appl. Phys. — 1950. — Vol. 21, no. 3. — P. 232–237.

10. Ostapenko V. V. Symmetric compact schemes with artificial viscosities of increased order of divergence // Comput. Math. Math. Phys. — 2002. — Vol. 42, no. 7. — P. 980–999.

11. Fiorina B., Lele S. K. An artificial nonlinear diffusivity method for supersonic reacting flows with shocks // J. Comput. Phys. — 2006. — Vol. 222. — P. 246–264.

12. Kawai S., Lele S. K. Localized artificial diffusivity scheme for discontinuity capturing on curvilinear meshes // J. Comput. Phys. — 2008. — Vol. 227, no. 22. — P. 9498–9526.

13. Kurganov A., Liu Y. New adaptive artificial viscosity method for hyperbolic systems of conservation laws // J. Comput. Phys. — 2012. — Vol. 231, no. 24. — P. 8114–8132.

14. Deng X., Maekawa H. Compact high-order accurate nonlinear schemes // J. Comput. Phys. — 1997. — Vol. 130, no. 1. — P. 77–91.

15. Deng X., Zhang H. Developing high-order weighted compact nonlinear schemes // J. Comput. Phys. — 2000. — Vol. 165, no. 1. — P. 22–44.

16. Jiang L., Shan H., Liu C. Weighted compact scheme for shock capturing // Int. J. Comput. Fluid Dyn. — 2001. — Vol. 15, no. 2. — P. 147–155.

17. Zhang S., Jiang S., Shu C.-W. Development of nonlinear weighted compact schemes with increasingly higher order accuracy // J. Comput. Phys. — 2008. — Vol. 227, no. 15. — P. 7294–7321.

18. Ghosh D., Baeder J. D. Compact reconstruction schemes with weighted ENO limiting for hyperbolic conservation laws // SIAM J. Sci. Comput. — 2012. — Vol. 34, no. 3. — P. A1678–A1706.

19. Guo Y., Xiong T., Shi Y. A positivity-preserving high order finite volume compact-WENO scheme for compressible Euler equations // J. Comput. Phys. — 2014. — Vol. 274. — P. 505–523.

20. Modified weighted compact scheme with global weights for shock capturing / Huankun Fu, Zhengjie Wang, Yonghua Yan, Chaoqun Liu // Comput. Fluids. — 2014. — Vol. 96. — P. 165–176.

21. Mikhailovskaya M. N., Rogov B. V. Monotone compact running schemes for systems of hyperbolic equations // Comput. Math. Math. Phys. — 2012. — Vol. 52, no. 4. — P. 578–600.

22. Rogov B. V., Mikhailovskaya M. N. Monotone high-accuracy compact running scheme for quasi-linear hyperbolic equations // Math. Models Comput. Simul. — 2012. — Vol. 4, no. 4. — P. 375–384.

23. Rogov B. V. Monotone bicompact scheme for quasilinear hyperbolic equations // Doklady Mathematics. — 2012. — Vol. 86, no. 2. — P. 715–719.

24. Rogov B. V. High-order accurate monotone compact running scheme for multidimensional hyperbolic equations // Comput. Math. Math. Phys. — 2013. — Vol. 53, no. 2. — P. 205–214.

25. Chikitkin A. V., Rogov B. V., Utyuzhnikov S. V. High-order accurate monotone compact running scheme for multidimensional hyperbolic equations // Appl. Numer. Math. — 2015. — Vol. 93. — P. 150–163.

26. Fedorenko R. P. The application of difference schemes of high accuracy to the numerical solution of hyperbolic equations // Comput. Math. Math. Phys. — 1962. — Vol. 2, no. 6. — P. 1122–1128.

27. Rogov B. V., Mikhailovskaya M. N. Monotone bicompact schemes for a linear advection equation // Doklady Mathematics. — 2011. — Vol. 83, no. 1. — P. 121–125.

28. Tolstykh A. I. Hybrid schemes with high-order multioperators for computing discontinuous solutions // Comput. Math. Math. Phys. — 2013. — Vol. 53, no. 9. — P. 1303–1322.

29. Sedov L. I. Similarity and dimensional methods in mechanics. — 10 edition. — CRC Press, 1993.